Study of the Behaviour of Moment-Resisting Connection of Softwood Timber Elements

Janis Fabriciuss[1)*], Lilita Ozola[2)]

[1)*] Institute of Civil Engineering and Wood Processing, Faculty of Forest and Environmental Sciences, Latvia University of Life Sciences and Technologies, 19 Akademijas Str, Jelgava, LV-3001, Latvia; email: janis.fabriciuss@lbtu.lv; ORCID: https://orcid.org/0009-0005-6385-4876

[2)] Institute of Civil Engineering and Wood Processing, Faculty of Forest and Environmental Sciences, Latvia University of Life Sciences and Technologies, 19 Akademijas Str, Jelgava, LV-3001, Latvia; ORCID: https://orcid.org/0000-0003-3766-6706

http://doi.org/10.29227/IM-2024-02-25

Submission date: *03.05.2024.* | Review date: *11.06.2024*

Abstract

Timber moment-resisting connections present opportunities for streamlined architectural design using timber portal frames with rigid knee junctions, enabling open floor plans by eliminating the need for additional bracing or interior columns. This flexibility empowers architects to craft more versatile floor layouts, enhancing spatial aesthetics and functionality. However, moment-resisting connections between timber members, especially crossing ones, present several challenges – complex design, demanding meticulous detailing and precise fabrication and also lack of a detail design format in codes. One of the biggest disadvantages of timber moment-resisting connections made by steel dowels is development of relative rotation due to the timber as well as dowel's elastic-plastic behaviour, i.e., such connection may be referred to a semi-rigid group. The main objective of this study is to conduct a detailed investigation of semi-rigid timber connections by performing experimental tests of L-shape models, including examination of timber strength and stiffness properties. The rotational displacement between joined members was determined using measured distances between surface points by Particle Image Velocimetry (PIV). The experimental results are compared with an equivalent linear calculation model. Different connection models are treated by Dlubal RFEM software tools using experimentally obtained embedment stiffness variables. It is found that the linear behavior of the semi-rigid connection is up to approximately 40% of the connection's design capacity, after which distinctly nonlinear force-deformation relationship develops.

Keywords: *Timber connection, Modulus of Elasticity, Particle image velocimetry, Semi-rigid, Performance-based design, FEM*

1. Introduction

Timber moment-resisting connections, when secured by mechanical fasteners, offer distinct advantages comparable to traditional timber pinned connections, such as enhanced structural stability, decreased displacement between structural members joined, and potential augmentation of load-bearing capacity within specific frame sections. Notably, they excel in withstanding lateral and seismic forces, ensuring structural integrity, particularly in seismic-prone areas or dynamic load environments, such as bridges. Moreover, moment-resisting connections present opportunities for streamlined architectural design using portal frames with rigid knee junctions, enabling open floor plans by eliminating the need for additional bracing or interior columns. This flexibility empowers architects to craft more versatile floor layouts, enhancing spatial aesthetics and functionality.

However, moment-resisting connections between timber members, especially crossing ones, present several challenges. Firstly, their calculations and design are inherently more intricate and time-consuming compared to pinned connections, demanding meticulous detailing and precise fabrication. Secondly, despite the fact that their bearing capacity is calculated and the connection is correctly designed according to the building code, moment-resisting connections do not exhibit full rigidity, so this type of connection is called semi-rigid. Depending on the specifics of connection, small rotations may occur a load is attached, leading to significant displacements at critical points such as apex point in portal frame. Thirdly, moment-resisting connections made by mechanical fasteners can promote a high stress concentration in wood near the fasteners. This phenomenon may result to local crack propogation in wood or overall connection failure, even when the applied load is below the bearing capacity. These factors underscore the importance of thorough analysis and careful consideration when implementing moment-resisting connections in timber structures.

2. Background

Previous research has indicated that a timber moment-resisting connection using steel fasteners may be assessed as a semi-rigid connection (Basterrechea-Arévalo etc., 2023),(Mehra etc., 2021) due to demonstration of some rotational deformability. A slight connection rotation is observed under designed service loads, which consequently affects not only the performance of the connection itself but also the overall system stability, especially if such a connection is used in a knee joint of portal frame. It is stated from consideration of static equilibrium that each couple of fasteners induce resisting moment, and the total resistance of the connection depends on the distance of the fastener from the connection center (Figure 1). Accordingly, if the fasteners are further from the connection center, the connection itself becomes much stiffer. Reactive forces acting to resist applied moment depend on diameter and number of the the fasteners. An adequate number of fasteners must be placed around the connection area to ensure that potential stresses do not exceed not only the bearing capacity of the fastener themselves but primarily not exceeding wood'

resistance along the fiber direction as well as in cross direction of fibers.

It is clear that rotation between timber members in moment-resisting connection primarily is caused by the following reasons:

- Fasteners in the connection are typically installed in pre-drilled holes, which diameter is usually larger than the fastener's diameter. Consequently, initial movement is possible within the connection until the fastener presses against the hole wall. This initial movement could potentially result in approximately 1 mm displacement per fastener in the connection.
- Due to the anisotropic nature of wood, the fastener meets different material stiffness when embeds into the crossing members connected, and the embedment deformation depends on the angle between reactive shear force transferred by bolt and fiber direction. If the reactive force acts in the timber fiber direction, the embedding into the wood will be less compared with the deformation caused by the reactive force acting perpendicular to the fiber direction. Note, that modulus of elasticity of softwood in fiber direction and perpendicular to fiber direction differ approximately 30 times (EN 338), which directly influences the behaviour of semi-rigid connection. In normal design practice, timber semi-rigid connections should be designed so that under service loads, the embedding into the timber does not exceed 0.5-1 mm.
- In a rationally designed connection, the bending deformation of the steel fastener also occurs in the design load range. Deformation is more pronounced when the load level exceeds 40%-50% of the total design capacity of a moment connection. In lower load levels, relatively small displacements are typically observed in the connection, meaning the connected elements are not sufficiently displaced angularly from each other, thus only the shear force created by the fastener needs to be compensated. As deformations increase, the fasteners begin to bend, leading to deformation of the fastener itself. It can be considered that under normal operating loads, fastener deformations should not exceed 0.5 mm displacement in one shear plane.

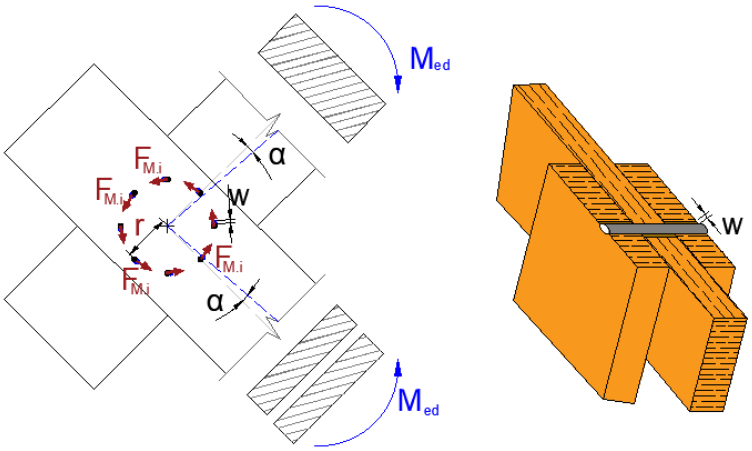

Fig. 1. Structural model of the L-type connection

In this study, behaviour of steel fasteners arranged in a circular shape will be examined. Fasteners are chosen to be placed only in one ring to clearly observe the action of each fastener under load. If the fasteners are arranged in the form of a ring, the center of the circle is taken as the center point of the joint, relative to which the moment equilibrium equation and experimentally determined angular displacements are established. Resisting to applied bending moment each fastener in such semi-rigid connection develops reactive force FM,i. Under designed service loads the moment equilibrium condition (formula (1)) should be satisfied. Previous assumptions (J. Porteous and A. Kermani 2013),(P.Racher 1995) indicate that the reactive forces are uniform distributed throughout the ring, provided that the distance to the connection centre remains unchanged.

$$M_{ed} = \sum_{n=1}^{\infty} F_{M,i} \cdot r, \tag{1}$$

where Med is external applied moment (kNm) and r is a radius measured form centre of connection till fasteners.

3. Materials And Methods

For the deepened study of behaviour of the semi-rigid connection, the L-type model was created considering size limitations for specimens in testing machines. To identify the fastener's performance under load, an examination is conducted analysing the fastener's embedment into wood for both parallel to the fiber direction and perpendicular to it, regarding essentially distinctive modulus of elasticity (MOE) values (E0 and E90). To specify the timber strength class, small specimens were made from the same softwood material as L-shape models, and a strength test was performed. Based on the obtained experimental results, an analytical calculation model is developed in Dlubal RFEM with the aim of approximation the analytical model to the experimental model.

Two models were made for the experimental tests in short-term static loading. The shape of model was selected according to the previous experimental experience. The selected shape of models is L-type. The model represents the connection of three timber boards – bottom column element is created with cross section 16.5×94.4mm and top beam element were made with cross section 41.7×94.7 mm (Figure 2). Each dowel-type fastener behave in double shear. Timber elements made of softwood lumber (spruce Picea Abies) with moisture content 6%. Wood around connection area was free of knots and cracks, the boards had straight fibers. Experimental test setup is shown in Figure 3. Model was painted with white paint and over white paint was sprayed black paint to create dotted surface with purpose to apply a new method for measurement of surface deformations. This method is based on PIV (Particle Image Velocimetry), which allows determining the movement of individual image fragments (Guedes at al, 2019).

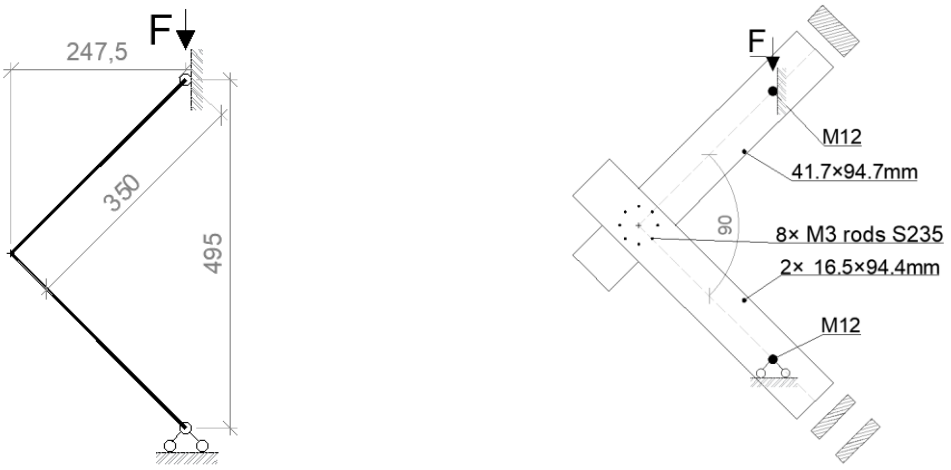

(a) (b)

Fig. 2. Experimental L-type model: a) design scheme; b) structural model

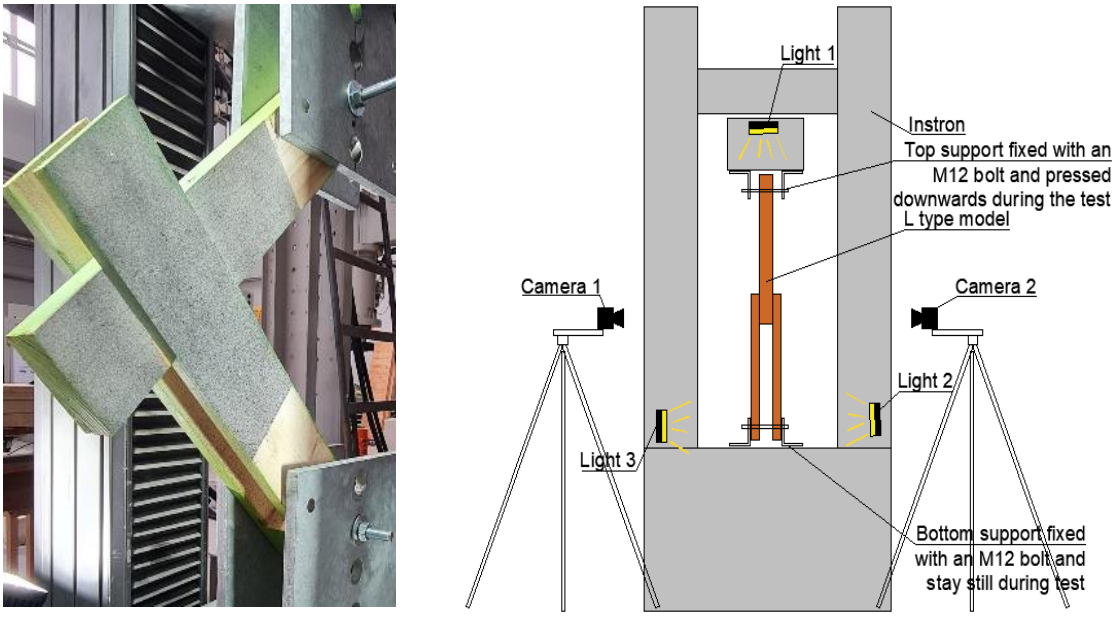

(a) (b)

Fig. 3. Test setup: a) experiment model painted to create dots on the surface; d) experiment setup.

Each model was subjected to temporary loading for up to ten minutes. Compression load as applied with speed 500N per minute. The load was applied incrementally, resulting in a total of 7 steps (Figure 4). The models were subjected to compressive loads. During loading, data were collected from two cameras, with each camera capturing deformations in the connection simultaneously (figure 3). Surface illumination - 600 lux. Photo fixation was performed with Sony a6400 cameras, and further photo processing was carried out in the ZEISS INSPECT correlate software.

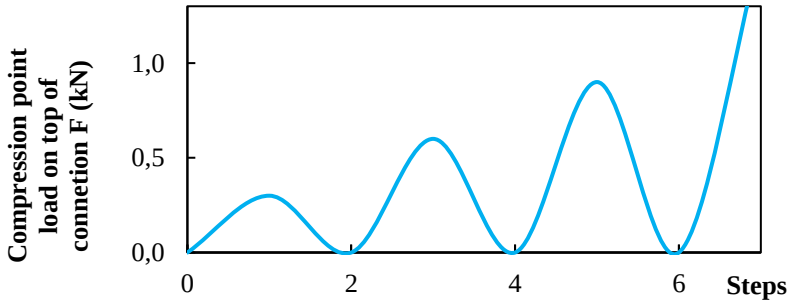

Fig. 4. Short-term load test setup.

To examine the embedment stiffness of wood, a total of 3 specimens were made to examine modulus of elasticity E90, and 11 specimens were created for the determination of MOE (E0) in the grain direction. A small number of specimens is explained by the additional need that arose during the testing process to clarify only one type of action of the fastener in connection, determining how this fastener presses into the wood. Specimens were created according to EN 383 requirements. Fastener – M6 steel rod,

strength class S235JR. Predrilled hole for fastener – 6 mm. Thickness of the specimen – 20 mm, width – 91 mm, length for small pieces ~93mm, large one was 240 mm.

Specimens were tested using universal testing machine INSTRON (Figure 5). To conduct loading tests, additional custom-made equipment was utilized. Tests were conducted under short-term loading. The testing regime is set at a head displacement of 1mm/min for the testing equipment. According to EN 383 standard, the test is performed until the total compression deformation into wood reaches 5 mm.

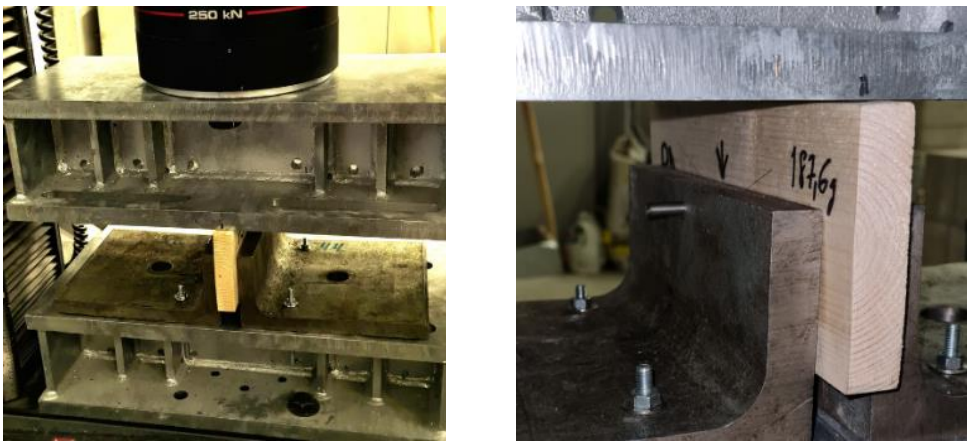

Fig. 5. Experiment setup for Elastic modulus for fiber direction E0 and perpendicular to fiber direction E90.

To determine the mechanical properties of the wood used in previously tested models, an additional analysis of bending strength properties is conducted. To achieve this, specimens were prepared from the long pieces (Figure 5) and subjected to four-point bending according to the standard EN 408 (Figure 6).

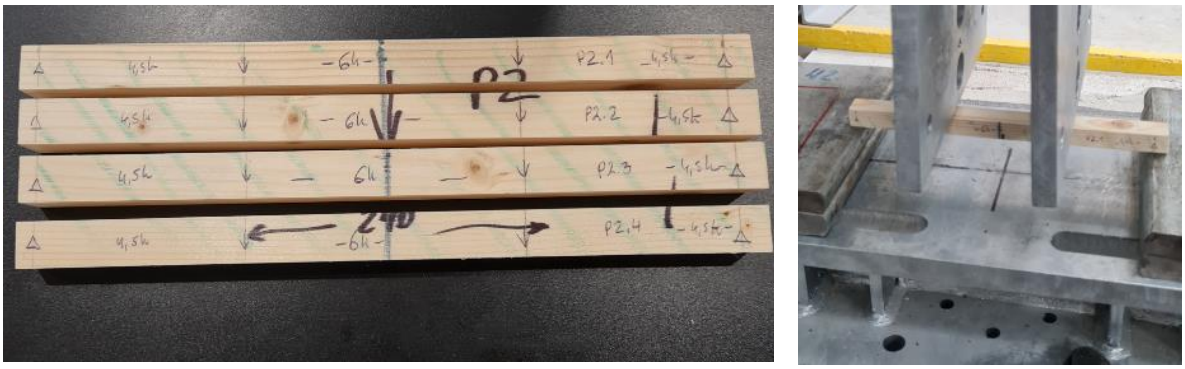

Fig. 6. Experiment setup 4 point bending test.

4. Results And Discussion

4.1. Bending strength and modulus of elasticity of wood

To ascertain the correct timber strength class, specimens were fabricated and static tests in four-point bending performed in accordance with standard EN 408. A total of 12 specimens were made, 235x20x15 mm. Upon conducting tests, the average bending strength was determined to be 48.8 ± 5.9 MPa. It should be noted that the timber used in the tests was stored in the laboratory warehouse, where the temperature fluctuates between 20±3°C, and the relative humidity is approximately 40-50%. The moisture content of the wood specimens was in the range 6-7%, thus the strength properties were reduced to 12% moisture content using known reduction coefficient. Data processing in accordance with the EN 14358 specifications proved, that the characteristic bending strength of timber specimens is 36.4 MPa. Furthermore, in accordance with EN 338 standard, the bending strength for softwood may be assessed as 35 MPa. Therefore, these selected specimens can be classified as of strength class C35 timber.

When conducting four-point bending tests, sufficiently high bending strength was established. Also, the MOE parallel to the wood fiber direction E0 was determined for all 12 beams. using values of mid-span deflection measured in the range of linear relationship with load. This displacement indicates not the overall deflection of the beams at mid-span, but the deflection at the points of applied load. The modulus of elasticity was collected during the linear stage of displacement increment. The overall modulus of elasticity was calculated using the full Mohr's integral, considering both deflection components caused by bending moment and shear force. Consequently, the average result for the modulus of elasticity is 6.94 ± 0.6 GPa. These MOE values correspond to the average values for C14 class timber according to the EN 338 standard.

Obtained results are illustrated by graphs in Figure 9 (b), representing the variability range of MOE (GPa) for timber specimens tested. Average Elastic modulus are 4-7 GPa.

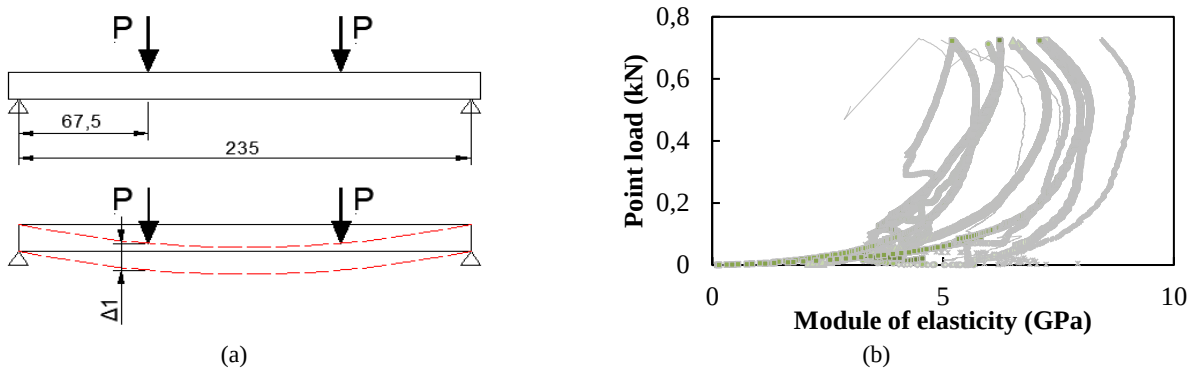

(a) (b)

Fig. 7. Experimental test setup for MOE: a) Test scheme; b) Variation of MOE depending on point load level

Summarizing the results of the bending strength tests and elastic properties of the timber specimens, it can be concluded that the bending strength of the wood is unexpectedly high, suggesting that the timber specimens used would belong to the C35 strength class. However, when evaluating the properties of the specimens in terms of elasticity, it must be noted that the selected specimens provide only the properties of C14 timber in terms of this indicator. Since the elastic properties of wood are crucial for moment resisting connections connected by dowels, it is further defined that the timber material is of C14 strength class.

4.2 Assessment of embedment stiffness of wood

When conducting a more in-depth analysis of the connection's behavior, the action of the dowels under load is analyzed. Here, the embedment of a steel dowel (diameter 6 mm) into the wood is examined. During the experiments, it was observed that when the dowel transfers a compression action along the fiber or perpendicular to the fiber direction, the deformations were significantly different. Up to 1 mm of total embedment deformation a good linearity between force and displacement was observed. Subsequently, as the load increased, the linear relationship became into non-linear. In the graphs (Figure 8), for comparison, a straight line characterizing the elastic properties of C14 timber strength class is indicated. The experimental results indicate that perpendicular to the wood fiber direction, the deformations observed are smaller than what would be expected for C14 timber. Accordingly, deformations observed parallel to the fiber direction in the experiment are larger. In this study embedment stiffness is characterised by embedment modulus defined as ratio of compression stress to relative deformation. In this case, the range of loading, where the measurements of embedment deformations were fixed, exceeds far from proportionality limits reaching up to 4.5 mm.

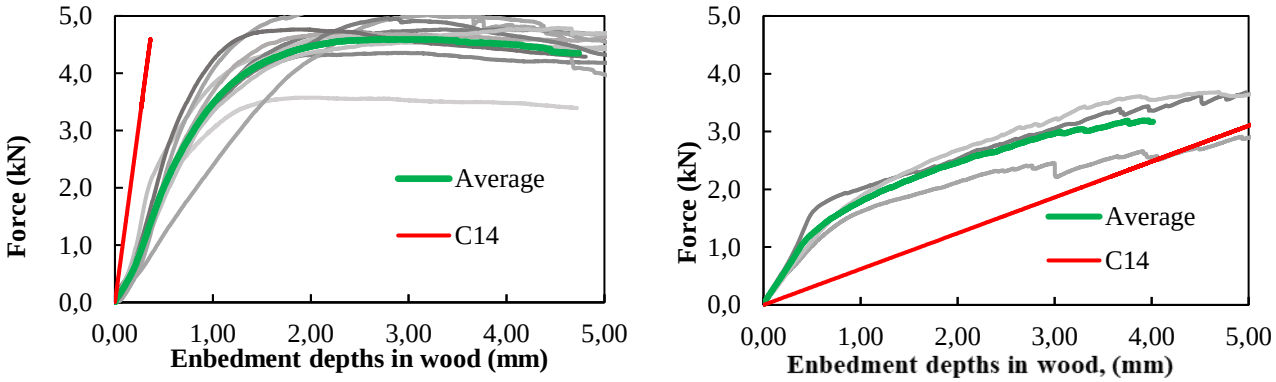

(a) (b)

Fig. 8. Development of embedment deformation versus force: a) in compression parallel to fiber direction; b) in compression perpendicular to the wood fiber direction.

The obtained results from Figure 8 are further summarized in Table 1. The table compiles the results of the embedment modulus. Since the results from Figure 8 indicate that as the load increases, the dowel embeds nonlinearly into the wood, then at a specific embedment (mm), the embedment modulus (GPa) is recorded. To determine the embedment modulus at 45 degrees, a generalized form of Hooke's Law is utilized for the orthotropic specimen with a fiber angle α (formula (2)), as described in the derivation (Kawahara, Ando, un Taniguchi 2015).

$$\frac{1}{E_{(\alpha)}} = \frac{1}{E_L}\cos^4\alpha + \left(-2\frac{\vartheta_{LT}}{E_L} + \frac{1}{G_{LT}}\right)\sin^2\alpha\cos^2\alpha + \frac{1}{E_T}\sin^4\alpha \quad (2)$$

Tab. 1. Embedment modulus in different load stages.

Stages - when are collected Elastic modulus (E)	Embedment modulus on different angle (GPa)		
	0	45a	90
0.5mm	12,9	9,2	8,3
1.0mm	11,7	8,5	5,9
1.5mm	9,2	6,9	4,9
2.0mm	7,4	5,5	4,2
2.5mm	6,2	4,6	3,7
3.0mm	5,1	3,8	3,3
3.5mm	4,4	3,3	2,9
4.0mm	3,8	2,9	2,6

a Elastic modulus on angle 450 where calculated according to results at fiber direction and perpendicular to the fiber.

4.3 Results of static tests of L-shape model

L-shape models were manufactured and placed in the loading device. Loading was carried out in the universal testing machine INSTRON. Data characterising the models' performance were collected by photographing them at specific load levels. The graphs in Figure 9(c) show the fixed distances between the surface points at certain load levels, which represent the real displacements between the pins. Graphs in Figure 9 (c) includes separate series L1 and L2, which represent real displacements (mm) between points. L1 denotes the distance between points P1 and P2, while L2 denotes the distance between points P3 and P4. Since the test was conducted stepwise, residual deformations are clearly observable at initial loads as well. Estimating the wood material as of C14 strength class, the total load capacity of the models is assumed to be F=1.45 kN. The moment resistance of connection is M=0.36kNm. According to the test results, it is found, that the models have force capacity on top support (figure 2a) Fmax=1.6kN, which is only 14% higher than the design load. In graphs (c) and (d), it can be seen that up to approximately 40% of the joint's load capacity, it's behaviour may be considered as stiff, with no noticeable rotation between connected members. After the 40% threshold, the joint's behaviour becomes markedly inelastic. Beyond the 110% threshold, the joint's behaviour is close to the plastic collapse expectations. It should be noted that no significant crack development was observed at ultimate load, and the loss of joint resisting ability was attributed to the fact that the dowels had undergone significant deformation and were pulled out of the holes.

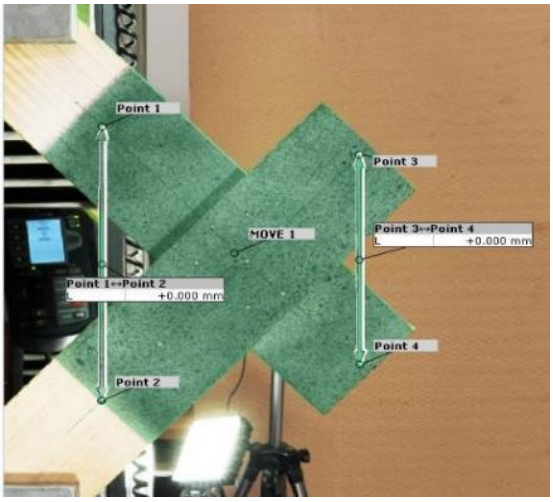

(a)

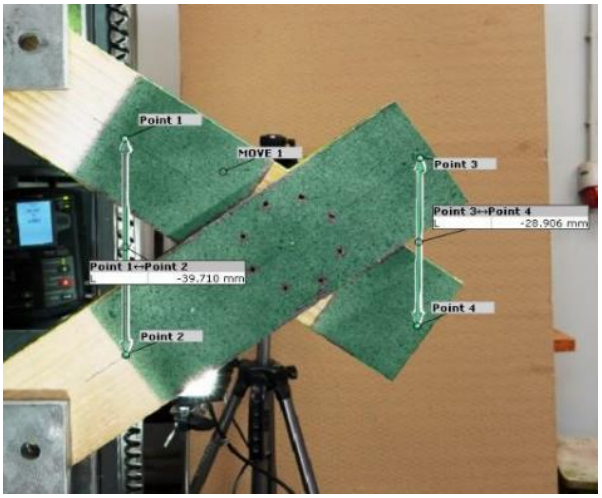

(b)

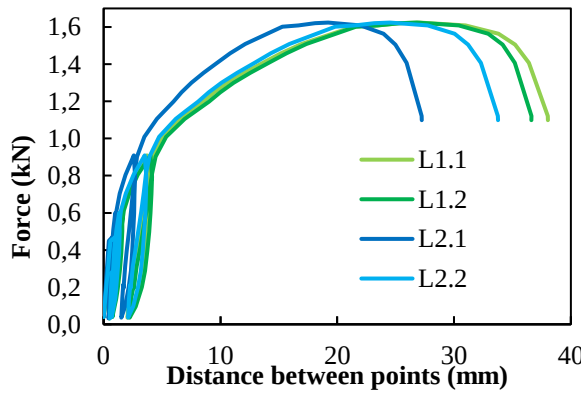

(c)

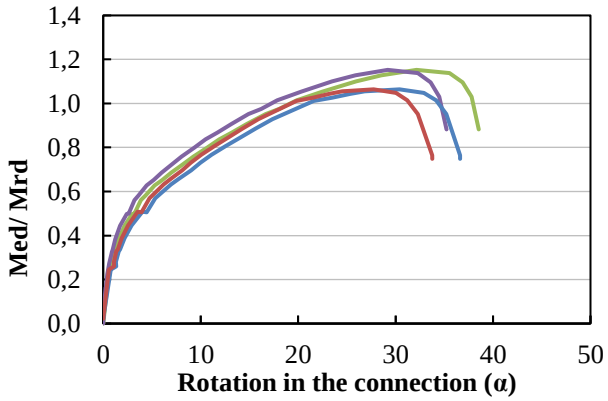

(d)

Fig. 9. L-shape model test: a) model fixed in machine and prepared for surface measurements; b) At the end of test; c) Relationships of surface deformations versus load, d) Relative moment capacity Med/MRd versus rotation between members

4.4 Results of treatment of theoretical model by RFEM

The analytical model of the L-type connection is simulated using the Dlubal RFEM software. analytical models were tested with purpose to understand the behavior of the experimental model and find the best fitted one. Since previous tests with single rod embedment in wood indicated that the modulus of elasticity for wood varies at different load levels and embedment depths, simulated springs elastic properties are created. Accordingly, simulations are conducted assuming that connection is fully rigid or its modulus of elasticity E corresponds to a 0.5 mm embedment, 1.0 mm embedment, etc. It is essential that the modulus of elasticity is also adjusted considering the reactive force direction against the wood's longitudinal fibers, according to Table 1. The results are indicated in graphs of Figure 10(b), where the relative moment capacity is plotted versus the connection's rotation. It is observed that up to 40% of the connection design load, the deformation of the dowels in the joint can be considered as negligible, corresponding to the case of fully rigid springs between steel dowels and drilled holes edges. Accordingly, above 40% of the load, there is a significant change has been demonstrated in the joint behavior, with a noticeable increase in dowels embedment in the wood, and further growth of deformation during the experiment even exceeds the predicted stiffness of connection which is observed when the rods embed in the wood up to four milimeters. In Figure 10(b), results of other simulation model from RFEM is included, where fictitious spring elements with defined nonlinear properties are defined in the drilled holes, exceeding the compression stress fixed at 15-17 MPa . For the simulation of the behavior of the behavior of connection it was assumed the possible range of modulus of elasticity from 60 MPa to 15 MPa. Note, that the values of the modulus of elasticity varies with change of an angle between shear force transferred by dowel and timber fiber direction. The resulting curve closely matches the experiment up to a load level of 40% of the connection design capacity, but beyond that, it is no longer representative.

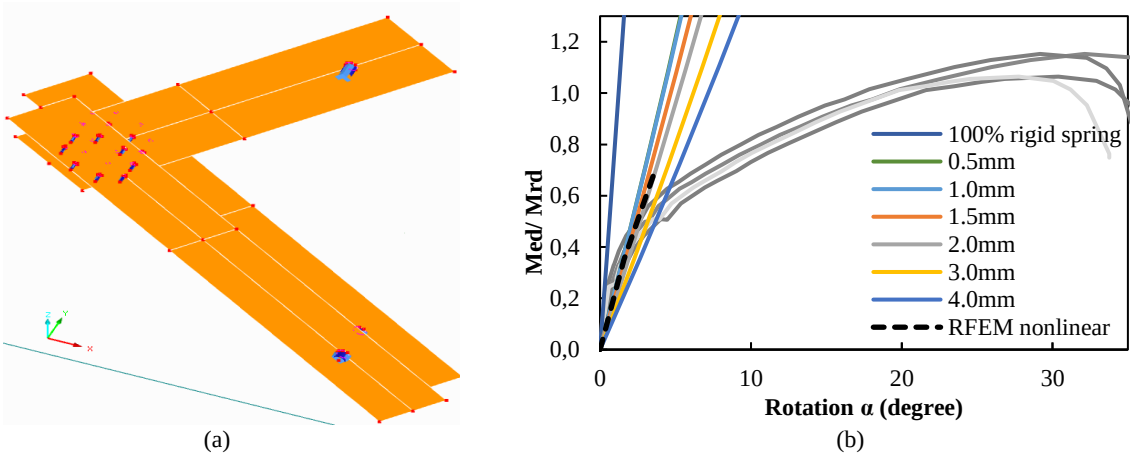

(a) (b)

Fig. 10. L-shaped model simulations in Dlubal RFEM and comparison of the obtained results with the experimental results: (a) Visualization of the RFEM model; (b) Obtained results from the experiment as well as stiffness simulation of the joint by varying the spring values.

When analyzing by Dlubal RFEM tools, it is observed that the internal reactive forces differ both for the middle wood member and for the outer elements. It is crucial that, despite using fundamentally identical springs oriented in the same direction with identical stiffness properties correspondingly the wood fiber direction, different reactive forces are obtained. The overall compiled graph is indicated in Figure 11(b), where all treated RFEM simulation models are summarized, and reactive forces are recorded for each model when an external force F=1 kN is applied at the upper node of the L-shaped model simulating the loading in the experiment. It is clear that the reactive forces at each simulated joint model are different, with larger reactive forces recorded in the middle element (marked as v), while the reactive force in the outer elements decreases by half, confirming the assumed theoretical basis (marked as a (Figure 11b)). Graphs in Figure 11(b) is also supplemented with theoretical values, external – 0,441 kN, internal – 0,882 kN reactive force. Analytical model shows average external reactive force 0,44±0.01 kN and internal 0,88±0.02 kN which are almost the same as theoretical. Looking at the maximum values, it is evident that the internal maximum reactive force is 1.04kN, which is 18% higher than it should be theoretically, and the external force is 0.54kN, which is 24% higher than theory predicts.

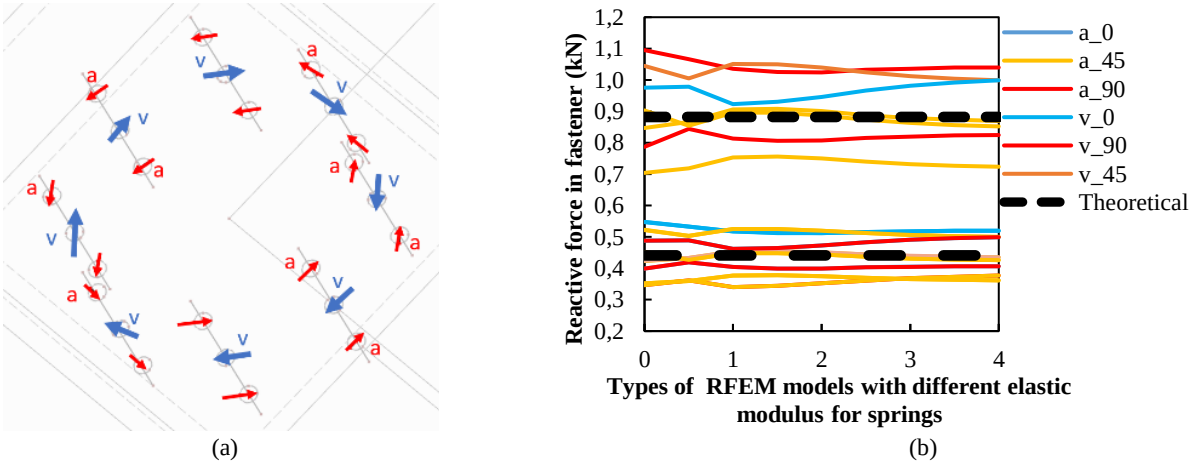

(a) (b)

Fig. 11. Visualization of internal reactive forces in the connection and an overall review of reactive forces for individual RFEM simulations: a) Visualization of reactive forces (v-forces in middle, a-forces in external element); b) Graphic of overall reactive forces in individual FEM simulations.

5. Conclusion

When conducting bending strength and modulus of elasticity tests on the wood samples used, insignificant differences were observed, and the bending strength properties of small samples with dimensions of 15x20 mm and a span of 235 mm indicated a C35 strength class using EN 408 standard guidelines. Additional investigation into the modulus of elasticity of wood revealed that the samples more closely align with the properties of the C14 strength class. In the authors' opinion, when determining wood properties, it is important to establish both strength and stiffness properties when strength class of timber is relevant.

Experiment results demonstrate differing deformations when the dowel transfers compression along or perpendicular to the wood fiber direction. Linearity between force and embedment deformation is observed in loading range producing deformation up to 3 mm along the fiber direction, while perpendicular to the wood fiber direction, linear relationships are observed up to 1 mm. Comparison of experimental results with the C14 strength class reveals that expected embedment modulus perpendicular to the fiber direction is higher, but lower against the fibers.

The L-type experimental models were tested using stepwise loading compression tests in the universal testing machine INSTRON. Connection deformation data were collected through photography and analyzed using Inspect Correlate software. The PIV method was employed to determine model displacements. Overall, linear deformations were observed in the models up to 40% of the total connection bearing capacity, followed by pronounced nonlinear deformation leading to collapse. The models' failure load was only 14% higher than the calculated bearing capacity, raising questions about the necessity of additional safety factors to reduce connection failure risk.

Analytical modeling in Dlubal RFEM software enable to simulate the behavior of L-shaped models under various conditions. The main task was to incorporate an original support conditions simulating of dowel embedment into wood. This was achieved by integrating small fictitious spring elements between the dowels and the edge of the wood hole, to which embedment modulus properties were assigned. The results indicate that the analytical model closely matches the experimental model up to 0.3-0.4 of the maximum connection bearing capacity. However, beyond this point, the experimental model exhibits distinctly plastic elasticity properties, which cannot be simulated using this type of model.

Analyzing the analytical model, it was observed that the reactive forces in each dowel are not equal and even differ among dowels oriented similarly to the wood fiber direction. This trend results in an uneven distribution of stresses in wood material throughout the connection area.

References

1. Basterrechea-Arévalo, M., M. Schweigler, R. Lemaître, un T. K. Bader, "Numerical modelling of moment-transmitting timber connections" (Engineering Structures, 2023), doi: 10.1016/j.engstruct.2023.116923.
2. Guedes, Taiane Oliveira, Rodrigo Allan Pereira, Fernando Pujaico Rivieira, un José Reinaldo Moreira da Silva " Particle image velocimetry for estimating the young's modulus of wood specimens" (Cerne, 2019), doi: 10.1590/01047760201925022633.
3. Kawahara, Ken, Kosei Ando, un Yusuke Taniguchi. "Time dependence of Poisson's effect in wood IV: influence of grain angle" (Journal of Wood Science, 2015), doi: 10.1007/S10086-015-1477-8/FIGURES/14.
4. Mehra, Sameer, Conan O'Ceallaigh, Adeayo Sotayo, Zhongwei Guan, un Annette M. Harte. "Experimental characterisation of the moment-rotation behaviour of beam-beam connections using compressed wood connectors " (Engineering Structures, 2021), doi: 10.1016/j.engstruct.2021.113132.
5. J. Porteous and A. Kermani. Structural timber design to Eurocode 5. (Chichester, West Sussex, UK: John Wiley & Sons Inc., 2013), 624 p.
6. H.J. Blaß, P. Aune, B.S. Choo, R. Görlacher, D.R. Griffiths, B.O. Hilson, P. Racher, G. Steck Timber Engineering. Step 1. (Netherlands: Centrum Hout, 1995)
7. European committee for standardization, EN 338:2021 Structural timber – Strength classes,(Avenue Marnix 17, B-1000 Brussels, 2016).
8. European committee for standardization, EN 408:2010+A1:2012 – Timber structures - Structural timber and glued laminated timber - Determination of some physical and mechanical properties,(Avenue Marnix 17, B-1000 Brussels, 2012).
9. European committee for standardization, EN 14358:2016 – Timber structures - Calculation and verification of characteristic values, (Avenue Marnix 17, B-1000 Brussels, 2016).